RSC Advances

The cellulose-based hydrogel which was prepared through glow discharge electrolysis plasma showed excellent swelling performance and multiple response behaviors.
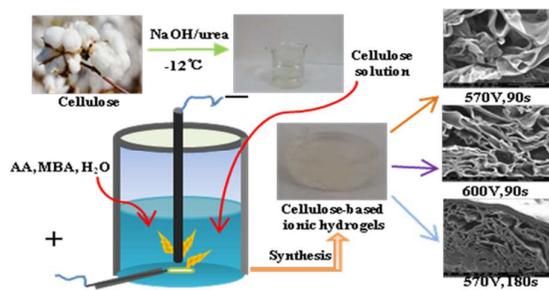
ARTICLE TYPE

Glow discharge electrolysis plasma induced synthesis of cellulose-based ionic hydrogels and their multiple response behaviors

Wenming Zhang,*[a] Zhu Sha,[a] Ying Huang,[a] Yunping Bai,[a] Ning Xi[a] and Yucang Zhang,*[b]

Novel ionic hydrogels were prepared successfully from cellulose in the NaOH/urea aqueous system by glow discharge electrolysis plasma (GDEP) technique. The structure and morphology of the ionic hydrogels were characterized by Fourier transform infrared spectroscopy (FT-IR) and scanning electron microscopy (SEM), as well as by determination of swelling and stimuli responses to pH and salts. The
10 results showed that the swelling behavior and the network structure of the ionic hydrogels could be controlled by changing discharge voltage or discharge time, whereas we obtained the maximum absorbency of 898 g/g for distilled water at 570 V and 90 s. Shrinkage of the network hydrogels took place at higher or lower pH. Relative to the Na^+ buffer solution, hydrogels exhibited more sensitive to Zn^{2+} and Fe^{3+} buffer solutions and showed network shrinkage and lower swelling ratio. This work
15 provided a new pathway for preparation of cellulose-based hydrogels with environmentally friendly, high water absorption capacity, rapid and multiple responses to pH and ions, which may allow their use in the biomaterials area.

KEYWORDS: glow discharge electrolysis plasma; cellulose; hydrogel; swelling ratio; response behavior

Introduction

20 Hydrogels, attractive soft materials, have received ever-increasing attention due to the applications in the fields of food, pharmaceuticals, agriculture, personal care products, and electronics[1]. Especially, biohydrogels are emerging as a potential alternative to synthetic hydrogels for the applications of
25 biomaterial field because of their unique advantages, such as abundance, non-toxicity, biocompatibility, biodegradability, and biological functions[2]. Recently, a great deal of attention has been diverted toward the production of biohydrogels from nature polymer, such as starch[3], cellulose[4], lignin[5], chitin/chitosan[6], and
30 agricultural wastes[7]. Among the numerous nature macromolecules used for hydrogel formation, cellulose is the most abundant natural polymer available worldwide. Besides, cellulose is inexhaustible source which could be considered as raw material of environmentally friendly and biocompatible
35 products[8] .
Recently, a novel solvent for the dissolution of pure cellulose in a precooled (-12 °C) 7wt% NaOH/12wt% urea aqueous solution have been developed and was considered a "green"

[a] College of Physics Science and Technology, Hebei University, Baoding,
40 *Hebei province, China. Fax: +86 312 5079473; Tel: +86 312 5079473;*
E-mail: wmzhang@hbu.edu.cn
[b] College of Materials and Chemical Engineering, Hainan University,
Haikou province, China. Fax: +86 898 66279219; Tel: +86 898
66279219; E-mail: yczhang@hainu.edu.cn

process[9]. Moreover, a series of initiated techniques have been proposed for the production of cellulose-based hydrogels, such as
50 chemical initiation, chemical cross-linking, UV-curing technique, microwave, and γ-ray irradiation[10]. However, these techniques have inherent disadvantages, such as less efficiency, high costs, and further generation of unwanted by-products or other toxic secondary pollution. Therefore, developing cheaper, higher
55 efficient, and "green" initiated technologies to enhance the performance of hydrogels are attracting considerable attention of scientists.
Glow discharge electrolysis plasma (GDEP) is emerging as a potential alternative to conventional technologies for the
60 formation of hydrogels due to its low costs, high efficiency, easy operation, and mild reaction conditions[11]. GDEP is a kind of non-faradaic electrochemical process and exhibits the characteristics of non-faraday, which produces numerous highly active particles in plasma electrolysis, such as HO•, H•, HO$_2$•, e_{aq}^-, and H_2O_2[12].
65 The yield of HO• is more than 12 mol per mole electron of electricity in the process of glow discharge electrolysis, which suggests that GDEP is a rich source of free radical in aqueous solution and can be applied to induce some unusual chemical reactions by taking place of chemical initiator in solution[13]. In
70 recent years, a series of adsorbing composites were prepared by GDEP technology and showed some excellent properties[14]. However, there were few studies directly on the preparation of cellulose-based hydrogels with multi-stimulus response properties by GDEP technology.
75 Acrylic acid (AA) is an important monomer that is widely used

for the production of functional hydrogels. Hydrogels can exhibit excellent responses to various external stimuli, such as pH and salts by incorporation of AA into the network, and thus allows their use in drug release systems[15]. In this study, we prepared novel ionic hydrogels based on cellulose in NaOH/urea aqueous system by introducing carboxyl groups into the network of hydrogels and using GDEP initiated technique. The effects of discharge parameters on the network structures of the prepared hydrogels were characterized, and the multi-stimulus responses to pH and salts were also investigated.

Experimental

Materials

Medical absorbent cotton of degree of polymerization 600 was bought in Hebei Baota Sanitary Materials Factory. NaOH, urea, NaCl, $ZnCl_2$, $FeCl_3$, acrylic acid (AA), N, N-methylene double acrylamide (MBA) were all analytically pure.

Experiment apparatus

The experimental apparatus consisted of a direct current power supply and a reactor, as shown in scheme. 1. The power supply was a LW100J1 DC power supply (Shandong, China) providing the voltage of 0-1000 V and the current of 0-1 A. The reactor was a cylindrical plexiglas chamber (Φ 30 mm×100 mm), containing a reflux condenser, a thermometer, a nitrogen conduit, a platinum anode with a diameter of 0.5 mm sealed into a glass tube to generate a glow discharge plasma in the aqueous solution, and a graphite cathode with a diameter of 10 mm. A magnetic stirring bar was placed at the bottom of the flask to keep the solution mixed well.
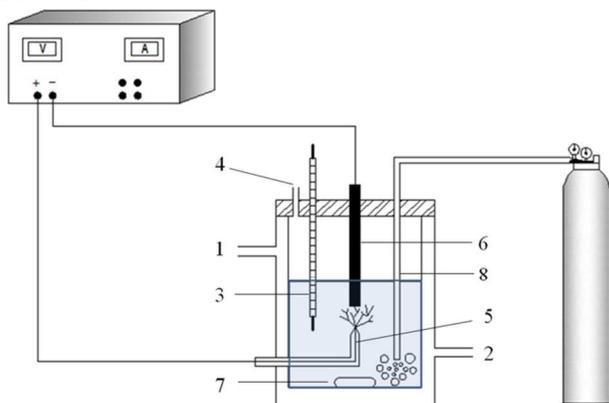
Scheme. 1 The experimental apparatus of the glow discharge electrolysis plasma. 1. cooling water outlet, 2. cooling water inlet, 3. thermometer, 4. gas outlet, 5. platinum wire, 6. graphite, 7. stirring pill, 8. gas inlet.

The preparation of cellulose-based ionic hydrogels

NaOH (7 g) and urea (12 g) were dissolved in distilled water (81 g) at -12 °C for 1 h, then cellulose (2 g) were added into the system with stirring rapidly, finally cellulose solution was obtained under the centrifugal effect. The above solution (10 mL) was carried into in the reactor as shown in Scheme. 1 with gaseous N_2. The glow discharge lasted 90 s with an applied voltage of 500 V, 540 V, 570 V, 600 V, 630 V and the glow discharge voltage kept 570 V with an applied discharge time of 30 s, 60 s, 90 s, 120 s, 180 s respectively. Then, 0.8 g AA and

0.02 g MBA were added to the system and stirring was continued for 2 h under N_2. The reaction was allowed to proceed at room temperature for 24 h. The hydrogels were carefully removed and washed thoroughly in distilled water for 7 days. During this period, the distilled water was replaced with fresh distilled water at least four times daily to leach out the NaOH excess. And COOH groups in the network hydrogels were converted to COO^- groups. The ionic hydrogels were dried to a constant mass at 60 °C.

Swelling measurement of cellulose-based ionic hydrogels

Preweighted dry hygrogels (m_d) were immersed into excessive distilled water to reach a state of equilibrium swelling at room temperature. The weight of the samples was monitored gravimetrically. The mass of the wet hydrogels (m_s) was determined after removal of the surface water by gently dabbing the hydrogels with filter paper. The water absorbency (SR) was calculated using the following equation:

$$SR = \frac{(m_s - m_d)}{m_d} \qquad (1)$$

where m_d and m_s are the weights of the preweighted dry hydrogel and the swollen hydrogel, respectively. SR is calculated as grams of water per gram of sample.

pH sensitivity of cellulose-based ionic hydrogels

The swelling ratios of the hydrogel samples were measured in pH of 1-12 using a gravimetric method. Test solutions with various pH values were prepared by combining HCl and NaOH properly, and the pH values were determined by a pH-meter (PHS-25, Shanghai Rex instrument Factory) at room temperature. The ionic strength of all the solutions was controlled to 0.1 mol L^{-1} using NaCl. Under the particular condition, the samples were incubated in the medium for at least 48 h and then removed, wiped with filter paper to remove water from the sample surfaces, and weighed. The swelling ratios of the hydrogels were expressed in terms of swelling ratio as formula (1).

Reversible switch response behavior of hydrogels: Dry hydrogel samples were immersed in buffer solution of pH=2.0 (off) until the swelling balance of hydrogels. At the same time, the weight and swelling ratio should be measured (weight of hydrogels was measured every 10 min until it came to a steady value) and then removed, wiped with filter paper to remove water from the sample surfaces. After that, the hydrogels were dipped in buffer solution of pH=7.0 (on) until hydrogels reached swelling banlance as well as the weight and swelling ratio would be measured. Reapeat these two steps, the hydrogels were put in buffer solution of pH = 2.0 (off) and pH = 7.0 (open). The circulation was made at least 3 times with new solution at every beginning of the cycle. According to formula (1), the swelling ratios were obtained.

Swelling measurement of cellulose-based ionic hydrogels in various salts solution

The balanced hydrogels were immersed into ionic buffer solution of Na^+、Zn^{2+} and Fe^{3+}. When the hydrogels reached balance, the weight and swelling ratio of the hydrogels were measured. Swelling ratios of the hydrogels were calculated through formula (1).

Morphology of cellulose-based ionic hydrogels

The cellulose-based ionic hydrogels were first immersed in distilled water to reach equilibrium swelling, and then the swollen hydrogel samples were freeze-dried. The morphology of the hydrogels was investigated by scanning electron microscopy (SEM, Quanta FEG). Specimens were coated with gold for 30 s in SEM coating equipment.

FT-IR analysis

FT-IR spectra of cellulose and cellulose-based ionic hydrogels were investigated by using Fourier Transform Infrared Spectrophotometer (Thermo Nicolet380). All measurements were carried out using the KBr disk technique.

Salt sensitivity of cellulose-based ionic hydrogels

The different hydrogels were immersed into ion buffer solution of NaCl, $ZnCl_2$, and $FeCl_3$ (0.5 mol L^{-1}). The weight and swelling ratio of hydrogels were measured when hydrogels came to balance. Formula (1) was the principle to calculate the swelling ratios.

Results and discussion

The mechanism of cellulose-based ionic hydrogels initiated by GDEP
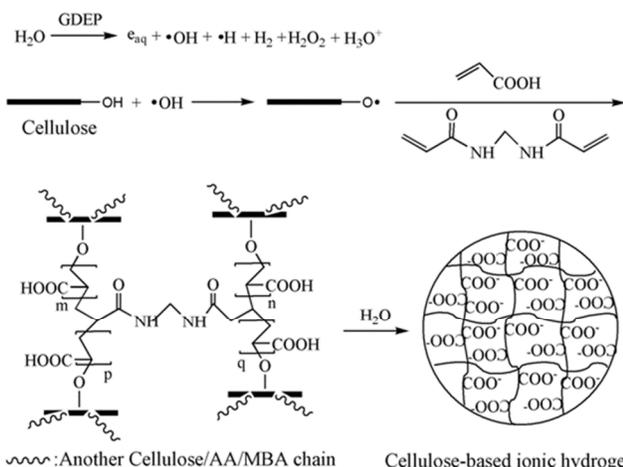
Fig. 1 Proposed mechanisms for synthesis of cellulose-based ionic hydrogels under GDEP (m, n, p, or q ≥ 1),

The proposed mechanistic pathway in the formation of synthetic adsorbent materials initiated by GDEP was described elsewhere[14]. Although there is no consistency about the formation of adsorbent composite by using GDEP technology, all agree that it follows free radical graft copolymerization process[16]. Specifically, the cellulose was dissolved in NaOH/urea (precooled at -12 °C) solution[17], then electrify the solution. At sufficiently high discharge voltage, water molecules absorb enough energy from plasma to form many energetic species including hydroxyl free radical. Afterwards, the energetic species attack further AA and cellulose molecules, forming the new AA and cellulose radicals, resulting in chain initiation and then themselves become free radical donors to the adjacent molecules to cause the chain propagation. The presence of cross-linking reagent (MBA) results in chains termination and a copolymer network comprising a cross-linked structure to prevent dissolution of the hydrophilic polymer chains in an aqueous environment. After the immersion of deionized water, the presence of COO^- groups on the polymer network enhance electrostatic repulsion, which favor the expansion of the chain network. The proposed mechanistic pathway in the formation of cellulose-based ionic hydrogels is shown in Fig. 1.

Influence of the discharge voltage and discharge time on swelling ratios of hydrogels
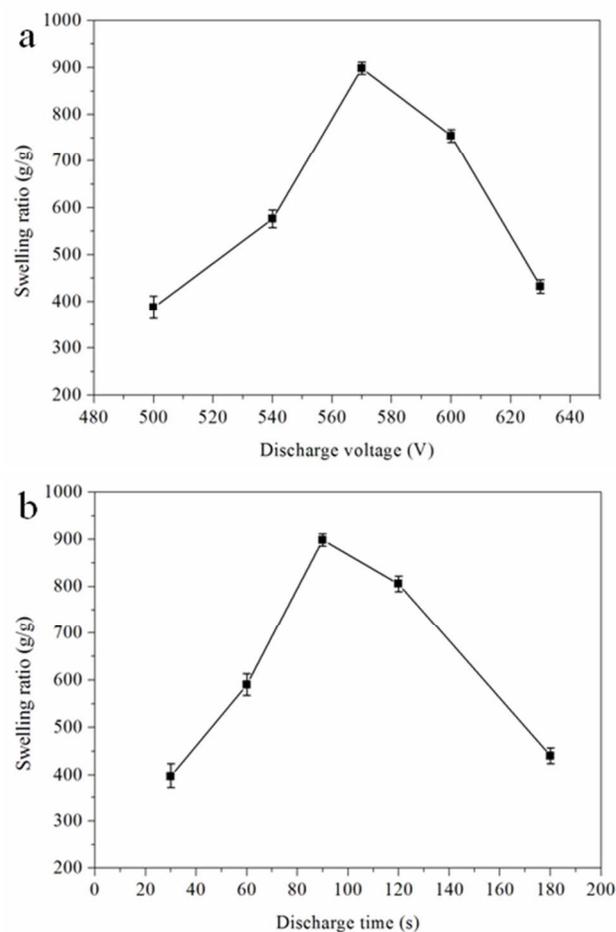
Fig. 2 Influence of discharge voltage and discharge time on the swelling behaviours cellulose-based ionic hydrogels in buffer solutions: (a) hydrogels with different discharge voltage (the discharge time was 90 s), (b) hydrogels with different discharge time (the discharge voltage was 570 V). The solutions were distilled water.

Fig. 2 (a) shows the influence of discharge voltage on swelling ratios of hydrogels. When the discharge voltage increased, the swelling ratios of hydrogels first increased and then decreased. The highest swelling ratio of hydrogels was 898 g/g when the discharge voltage was 570 V, which was higher than hydrogels prepared by chemical initiation[18]. This result is caused by the following conditions: when the discharge voltage is lower, the number of active particles is less, and copolymerization is incomplete due to bits of hydroxyl free radical. Then the short-chain polymer is formed, and the viscosity is higher. Thus, the swelling ratio is lower. When the discharge voltage exceeds 570 V, the polymerization reaction ratio accelerates due to numerous free radicals. Thereafter, polymer chain intertwines, resulting in a decline in water regain of hydrogel and a decrease in the swelling

ratio.

Fig. 2 (b) shows the influence of the discharge time on the swelling ratios of hydrogels. With the increase of discharge time, the swelling ratios first increased and then decreased. A shorter or
5 longer discharge time can cause a lower swelling ratio. In shorter discharge time, insufficient free radicals leaded to incomplete polymerization reaction which resulted in high viscosity and partial water solubility. By contrast, given the presence of abundant monomers and radicals of chains at a longer discharge
10 time, homopolymerization and chain termination reaction could be enhanced, thereby causing a denser network and a decrease in swelling ratio.

pH sensitivity of cellulose-based hydrogels
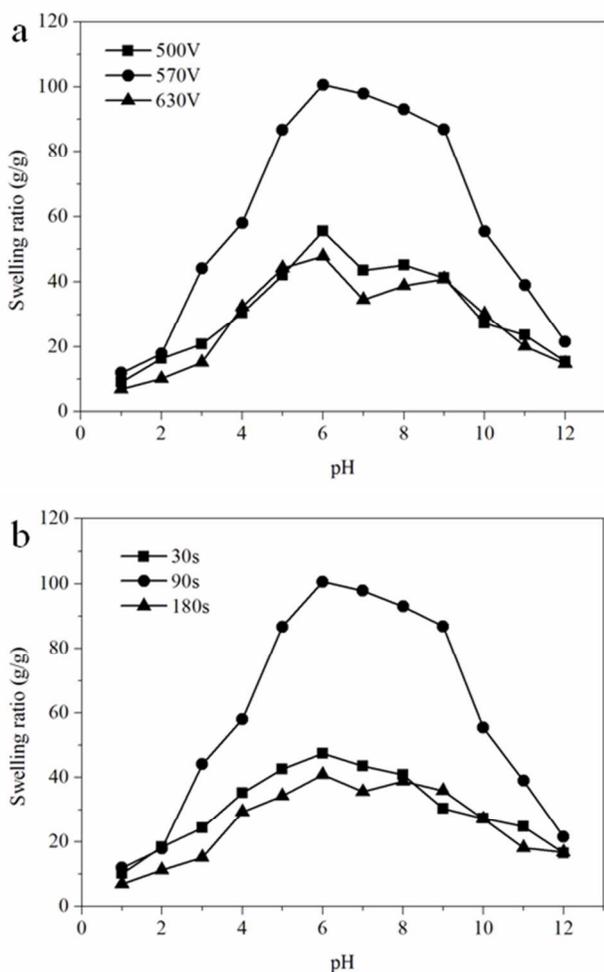
15 **Fig. 3** Effects of pH on the swelling behaviors of cellulose-based ionic hydrogels in buffer solutions: (a) hydrogels with different discharge voltage (the discharge time was 90 s), (b) hydrogels with different discharge time (the discharge voltage was 570 V). Ionic strengths of all solutions were controlled to 0.1 mol L^{-1} using NaCl.

20 Fig. 3 showed the influence of pH on the swelling ratios of hydrogels. Fig. 3 (a) illustrated that the water absorption swelling ratio of three types of hydrogels which were made under different voltages increased faster at $1 < pH < 6$ and reached the maximum at pH of 6. Then swelling ratio decreased slowly at $6 < pH < 9$,
25 finally swelling ratio dropped rapidly when $pH > 9$. These may be caused by the pKa value of the carboxylic group, which are 4.6.

The COO$^-$ groups are protonated to COOH gradually at lower pH (< 4.6), then decrease of electrostatic repulsion among COO$^-$, shrinkage of hydrogels network and lower swelling ratio are
30 caused by the protonation of COO$^-$. In addition, the ionization of COOH groups occurs at pH > 4.6, resulting in the expansion of the hydrogel network. Thereafter, the electrostatic repulsion is enhanced, and the swelling ratio increases. However, when the pH > 9, electrostatic shielding is caused by excessive Na$^+$,
35 leading to a decrease in the electrostatic repulsion between the COO$^-$. Subsequently, the swelling ratio rapidly drops. Fig. 3 (b) showed the water absorption swelling ratio of three types of hydrogels which were made in different discharge times. These hydrogels have different swelling ratios, but trends are all after
40 the first cut increased. The reason may be the incomplete polyreaction of the system. Homopolymerization and chain termination reaction could be enhanced because of abundant monomers and radicals of chains at a longer discharge time, resulting in a denser network and lower swelling ratios. Fig. 3
45 also showed that the swelling ratio of hydrogels was relatively low in different pH buffer solutions which are made in higher or lower discharge voltage system and shorter or longer discharge time. This result may be related to their incomplete copolymerization in the low voltage and high cross-linking
50 density.

On–off reversible switch behavior of cellulose-based ionic hydrogels
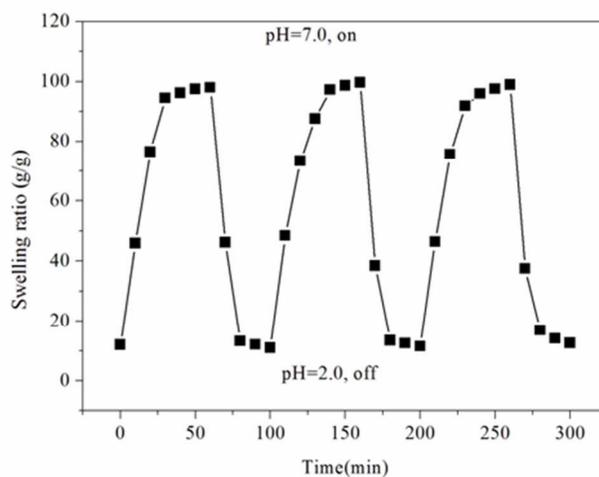
Fig. 4 On-off reversible switch behaviors of the cellulose-based ionic
55 hydrogel when the hydrogel was repeatedly immersed in buffer solutions of pH 2.0 and 7.0 (hydrogel with the discharge voltage and discharge time was 570 V and 90 s, respectively). Ionic strengths of all solutions were controlled to 0.1 mol L^{-1} using NaCl.

Given that cellulose-based ionic hydrogels showed different
60 response behaviors in different pH buffer solutions, a reversible switch is manufactured by using the feature, which was controlled by pH, was considered in this study. Fig. 4 shows the reversible switch response behavior of the pH control. The fig. 4 revealed that the carboxyl groups of hydrogels were protons in
65 pH = 2.0 buffer and electrostatic repulsion abated. The network structure also contracted. The volume became smaller, and the swelling ratios decreased. The switch, which exhibited intelligent response behavior, could still be observed after three cycles.

Therefore, cellulose-based hydrogels can be used as intelligent "on–off" in the future.

Salt response behaviors of cellulose-based ionic hydrogels
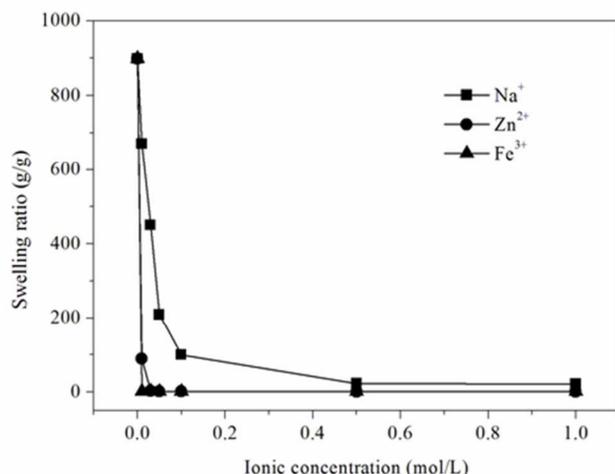
Fig. 5 Swelling ratio of cellulose-based ionic hydrogel in NaCl, ZnCl$_2$, and FeCl$_3$ solutions (hydrogel with the discharge voltage and discharge time was 570 V and 90 s, respectively). The solutions were distilled water. Fig. 5 shows the swelling ratios of hydrogels in the buffers of different salt types and concentrations. When the concentrations of Na$^+$, Zn^{2+}, and Fe^{3+} increased, the swelling ratios decreased, and the volume shrank until it reached a stable value. These results are caused by the different osmotic pressure inside and outside of network in different solutions. The ratio between the internal COO$^-$ and external positive ions of solutions are reduced by the increase of positive ion density, thereby the osmolarity decreases and the network contracts. At the same time, with the increase of electrolyte solution concentration, electrostatic shielding effect on the COO$^-$ of hydrogels is produced by Na$^+$, Zn^{2+}, and Fe^{3+}. This process results in lower electrostatic repulsion and contraction of the network, thereby reducing the swelling ratio. Fig. 5 also shows the ion species influence on the swelling behavior of hydrogels. The swelling ratio in Zn^{2+} and Fe^{3+} buffer solutions was lower than that in Na$^+$ buffer solution, indicating that the hydrogels were more sensitive to higher positive ions. The reason may be that higher positive charge makes the electrostatic shielding stronger and has larger effects on the network structure of the hydrogel and higher coordination effects between ions and carboxyl groups (Figure S3). However, the cation Na$^+$, as well as the swelling ratio, is the weakest.

Microstructure characterization of cellulose-based hydrogels
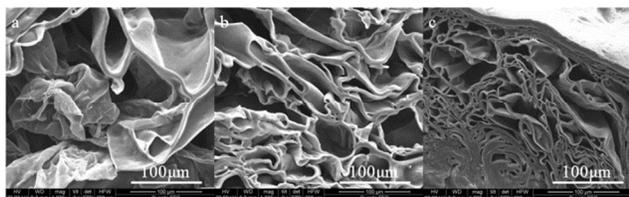
Fig. 6 The SEM micrographs of cellulose-based ionic hydrogels: (a) 570 V and 90 s, (b) 630 V and 90 s, and (c) 570 V and 180 s.

Fig. 6 shows the scanning electron microscopy (SEM) images of hydrogels at different discharge voltages: (a) 570 V, (b) 630 V, and different discharge times: (a) 90 s, (c) 180 s. The SEM images (Fig. 6) showed that all hydrogels consisted of three-dimensional network structures and a large number of miniature pores. Supposedly, these pores are the regions of water permeation and interaction sites of external stimuli with the hydrophilic groups of the graft copolymers. The micro holes of sample (a) were significantly larger than sample (b) microporous aperture. This result is caused by the condition wherein the increase of discharge voltage produces too many free radicals, inhibiting the formation of free radicals that cause long chain and decreasing the graft copolymerization reaction. Furthermore, some side effects, such as homopolymerization, occurred, resulting in the densification of the network structure and decrease in reservoir pore. This result also proved that cellulose-based hydrogel, preparation under higher voltage, exhibited a lower swelling ratio. In addition, the SEM images indicated that sample (c) had a less expanded network than sample (a) did. The homopolymerization and chain termination reaction could be enhanced because of the presence of abundant monomers and chain radicals at a longer discharge time. Thus, the network is denser, and the swelling ratio is less.

Structure characterization of cellulose-based ionic hydrogels
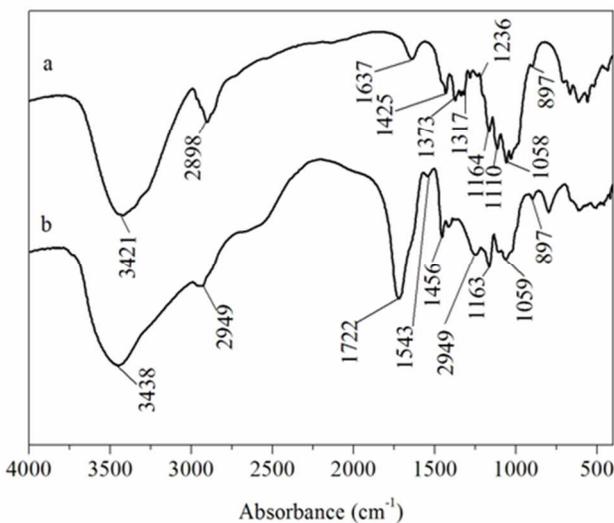
Fig. 7 FT-IR spectra of (a) cellulose and (b) cellulose-based ionic hydrogel.

Fig. 7 shows the infrared spectrogram of cellulose and cellulose-based ionic hydrogel. In the curve (a), the peaks at 3421 and 2898 cm^{-1} were associated with the –OH, –CH or –CH$_2$ groups stretching vibration, respectively. The bending vibration of the H–O–H of water absorption, –CH$_2$, C-H groups from cellulose appeared at 1637, 1425, 1317 and 1373 cm^{-1}, respectively. The absorbances at 1236, 1164, 1110, 1058 and 897 cm^{-1} were assigned to the C–O-C, C=O, glycosidic bond stretching vibration, respectively. As for spectra (b), new peaks at 1722, 1543, and 1456 cm^{-1} were related to the stretching vibration of C=O and COO$^-$. These results indicated that AA monomers were grafted onto the backbone of cellulose, connecting the cellulose groups to generate cellulose-based ionic hydrogel material.

Salt sensitivity of cellulose-based hydrogels

Fig. 8 shows the swelling ratios of hydrogels in different salt solutions (0.5 mol L^{-1}): NaCl, ZnCl$_2$, and FeCl$_3$. The hydrogels revealed different swelling behaviors in different salt solutions.
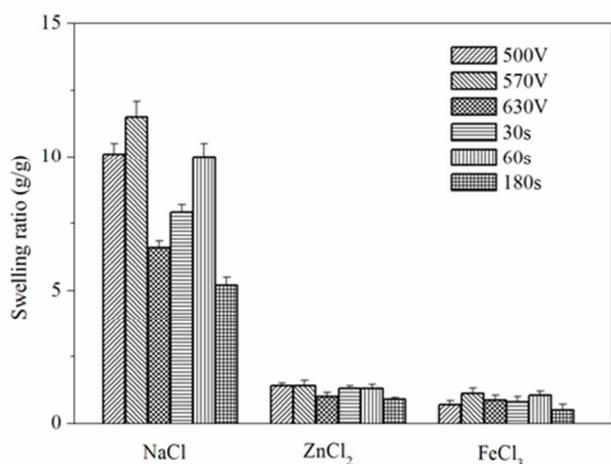
Fig. 8 Swelling ratio of cellulose-based ionic hydrogels in different salt solutions (0.5 mol L^{-1}), NaCl, ZnCl$_2$, and FeCl$_3$.

When the ionic types increased, the shrinking trend of the hydrogels also increased. The maximum swelling ratio was in NaCl solution, and the minimum value was in FeCl$_3$ solution. The swelling ratios of different hydrogels in NaCl solution were generally higher than those in ZnCl$_2$ and FeCl$_3$ solutions. Moreover, the ionic types (Zn^{2+} and Fe^{3+}) only slightly influenced the shrinking behavior of the six samples. Given the much stronger ionic cross-linking and charge screening effect, the significant differences among the six samples of hydrogels in 0.5 mol L^{-1} ZnCl$_2$ or FeCl$_3$ solution cannot be determined, and the swelling ratios were all small. The network of hydrogels is more sensitive to bivalent Zn^{2+} or trivalent Fe^{3+}. Therefore, the swelling behavior of hydrogels is intelligent in NaCl, ZnCl$_2$, and FeCl$_3$ aqueous solutions.

Conclusions

In summary, the GDEP was applied in aqueous solutions with MBA to prepare cellulose-based ionic hydrogels. SEM proved characterization of hydrogels with spatial three-dimensional structure. Hydrogels that are prepared under different discharge times and discharge voltages have various swelling ratios. The highest swelling ratio of hydrogels was 898 g/g when the discharge voltage was 570 V and the discharge time was 90 s. Hydrogels under different discharge times and voltages showed different response behaviors to the change of pH, ionic species, and concentrations. In the higher and lower pH buffer solutions, the network structure of hydrogels shrink and swelling ratio decreased. The volume shrink and swelling ratio of hydrogels decreased to a constant value when the ionic concentration of Na$^+$, Zn^{2+}, and Fe^{3+} increased. However, hydrogels were more sensitive to the same ion concentration of Zn^{2+} and Fe^{3+}. Their swelling ratios were also lower than those of the Na$^+$ buffer solution. The shrinking trend of different hydrogels showed different swelling ratios in the same ionic solution. The ionic types (Zn^{2+} and Fe^{3+}) exhibited a very slight influence on the swelling ratio of hydrogels, which was mainly attributed to the much stronger ionic cross-linking and charge screening effect. In Na$^+$ ionic solution, the swelling ratios of hydrogels are higher and more different. Furthermore, the hydrogels showed a reversible

on–off switching behavior in acidic–neutral solutions. These smart hydrogels will have wide applications, such as in agriculture, food, and drug delivery.

Note and references

1   Bingö B., Strandberg C., Szabo A., Wegner G., Macromolecules, 2008, 41, 2785–90.
2   (a) Cavalieri, F., Chiessi, E., Finelli, I., Natali, F., Paradossi, G., Telling, M. F., Macromolecular Bioscience, 2006, 6, 579–589; (b) Prabaharan, M., Mano, J. F., Macromolecular Bioscience, 2006, 6, 991–1008; (c) Yu, H., Lu, J., Xiao, C., Macromolecular Bioscience, 2007, 7, 1100–1111; (d) Zhai, M., Yoshii, F., Kume, T., Hashim, K., Carbohydrate Polymers, 2002, 50, 295–303 (e) Chang, C. Y., Duan, B., Cai, J. and Zhang, L. N., European Polymer Journal, 2010, 46, 92-100.
3   Dong, A. Q., Xie, J., Wang, W. M., Yu, L. P., Liu, Q., Yin, Y. P., J. Hazard. Mater., 2010, 181, 448−454.
4   O'Connell, D. W., Birkinshaw, C., O'Dwyer, T. F., A review. Bioresour. Technol., 2008, 99, 6709−6724.
5   Wu, Y., Zhang, S. Z., Guo, X. Y., Huang, H. L., Bioresour. Technol., 2008, 99, 7709−7715.
6   Kannamba, B., Reddy, K. L., AppaRao, B. V., J. Hazard. Mater., 2010, 175, 939−948.
7   Kadirvelu, K., Kavipriya, M., Karthika, C., Radhika, M., Vennilamani, N., Pattabhi, S., Bioresour. Technol. 2003,87, 129−132.
8   (a) Klemm D., Schumann D., Udhardt U., Marsch S., Prog Polym Sci, 2001, 26, 1561–603. (b) Klemm D., Schumann D., Cellulose, 2008, 15, 359–60. (c) Koschella A., Heinze T., Klemm D., Macromol Biosci, 2001, 1, 49–54. (d) Klemm, D., Heublein, B., Fink, H.P., Bohn, A., Angewandte Chemie International Edition, 2005, 44, 3358–3393. (e) Rinaudo, M., Progress in Polymer Science, 2006, 31, 603–632.
9   (a) Zhou, J., Zhang, L., Polym J, 2000, 32, 866–70. (b) Cai, J., Zhang, L., Liu, S., Liu, Y., Xu, X., Chen, X., Macromolecules, 2008, 41, 9345–51.
10 (a) Essawy, H. A., Ibrahim, H. S., React. Funct. Polym., 2004, 61, 421-432. (b) Peng, X. W., Ren, J. L., Zhong, L. X., Peng, F., Sun, R. C., Agric. Food Chem., 2011, 59, 8208-8215. (c) Peng, X. W., Zhong, L. X., Ren, J. L., Sun, R. C., J. Agric. Food Chem., 2012, 60, 3909-3916. (d) Sen, G., Singh, R. P., Pal, S., J. Appl. Polym. Sci. 2010, 115, 63-71. (e) Sun, J. Y., Zhao, X.H., Illeperuma, W. K., Chaudhuri, O., Oh, K. H., Mooney, D. J., Vlassak, J. J., Suo, Z, G., Nature, 2012, 489, 133-136.
11 (a) Gao, J. Z., Yu, J., Li, Y., He, X. Y., Bo, L. L., Pu, L. M., Yang, W., Lu, Q. F., Yang, Z. M., J. Hazard. Mater. B 2006, 137, 431-436. (b) Gao, J. Z., Li, Y. P., Li, Y., Liu, H. W., Yang, W., Cent. Eur. J. Chem., 2012, 10, 1766-1772. (c) Wang, X. G., Gao, J. Z. and Yang, W., Polymer Engineering and Science, 2012, 52, 2217-2227
12 (a) Lu, Q. F., Yu, J., Gao, J. Z., J. Hazard. Mater., B 2006, 136, 526-531. (b) Sengupat, S. K., Singh, O. P., J. Electroanal. Chem., 1994, 369, 113-120. (c) Sengupat, S. K, Singh, R., Srivastava, A. K, J. Electrochem. Soc., 1998, 145, 2209-2213. (d) Sengupta S. K., Sandhir U., Misra N., J. Polym. Sci. A: Polym. Chem., 2001, 39, 1584-1588.
13 (a) Lu, Q. F., Yu, J., Gao, J. Z., Yang, W., Li, Y., Plasma Process. Polym., 2011, 8, 803-814. (b) Yu, J., Pan, Y. P., Lu, Q. F., Yang, W., Gao, J. Z., Li, Y., Plasma Chem. Plasma P., 2013, 33, 219-235.

(c) S. K. Sengupta, R. Singh, A. K. Srivastava, Indian J. Chem., 1998, A37, 558.

14 (a) Gao, J. Z., Wang, A. X., Li, Y., Fu, Y., J. Wu, L., Wang, Y. D., Wang, Y. J., React. Funct. Polym., 2008, 68, 1377. (b) Gao, J. Z.,
5   Ma, D. L., Lu, Q. F., Li Y., Li, X. F., Yang, W., Plasma Chem. Plasma Process., 2010, 30, 873.

15 (a) Chen, Y. J., Hazard. Mater., 2009, 171, 802–808. (b) Guclu, G., Gurdag, G., Ozgumus, S. J. Appl., Polym. Sci., 2003, 90, 2034–2039. (c) Keles, S., Guclu, G., Technol. Eng., 2006, 45, 365–371.
10   (d) Liu, F., Luo, X. G., Lin, X. Y., Liang, L. L., Chen, Y., J. Hazard. Mater., 2009, 171, 802–808. (e) Qiu. X. Y. and Hu, S. W., Materials, 2013, 6, 738-781. (f) Sannino, A., Demitri, C. and Madaghiele, M., Materials, 2009, 2, 353-373.

16 (a) Liu, Z. L., Hu, H., Zhou, R. X., J. Polym. Sci., Part A: Polym.
15   Chem., 2004, 42, 4370–4378. (b) Mahdavinia, G. R., Pourjavadi, A., Hosseinzadeh, H., Zohuriaan, M. J., Eur. Polym. J., 2004, 40, 1399–1407. (c) Pourjavadi, A., Harzandi, A. M., Hosseinzadeh, H., Modified carrageenan 3, Eur. Polym. J., 2004, 40, 1363–1370. (d) Gurdag, G., Yasar, M., Gurkaynak, M., A. J. Appl. Polym. Sci.,
20   1997, 66, 929–934.

17 (a) Chang, C. Y. and Zhang, L. N., Carbohydrate Polymers, 2011, 84, 40–53.

18 (a) Wu, F., Zhang, Y., Liu, L. and Yao, J.M., Carbohydrate Polymers, 2012, 87, 2519-2525.